Cellular Physiology and Biochemistry

Cell Physiol Biochem 2018;51:589-609
DOI: 10.1159/000495280
Published online: 20 November 2018
Accepted: 12 November 2018

Original Paper

Intrinsic Surface Effects of Tantalum and Titanium on Integrin α5β1/ERK1/2 Pathway-Mediated Osteogenic Differentiation in Rat Bone Mesenchymal Stromal Cells

Mengmeng Lu[a] Xiaohua Zhuang[b] Kaiwei Tang[c] Peishi Wu[c]
Xiaojing Guo[a] Linling Yin[a] Huiliang Cao[c] Derong Zou[a]

[a]Department of Stomatology, Shanghai Jiao Tong University Affiliated Sixth People's Hospital, Shanghai, [b]Department of Stomatology, Gongli Hospital, Second Military Medical University, Shanghai, [c]State Key Laboratory of High Performance Ceramics and Superfine Microstructure, Shanghai Institute of Ceramics, Chinese Academy of Sciences, Shanghai, China

Key Words
Tantalum • Titanium • Metal oxide • Integrin α5β1 • Osteogenesis

Abstract
Background/Aims: Accumulating evidence demonstrates the superior osteoinductivity of tantalum (Ta) to that of titanium (Ti); however, the mechanisms underlying these differences are unclear. Thus, the objective of the present study was to examine the effects of Ta and Ti surfaces on osteogenesis using rat bone mesenchymal stromal cells (rBMSCs) as a model. ***Methods:*** Ta and Ti substrates were polished to a mirror finish to minimize the influences of structural factors, and the intrinsic surface effects of the two materials on the integrin α5β1/mitogen-activated protein kinases 3 and 1 (ERK1/2) cascade-mediated osteogenesis of rBMSCs were evaluated. Alkaline phosphatase (ALP) activity, Alizarin Red staining, real-time polymerase chain reaction, and western blot assays of critical osteogenic markers were conducted to evaluate the effects of the two substrates on cell osteogenesis. Moreover, the role of the integrin α5β1/ERK1/2 pathway on the osteoinductive performance of Ta and Ti was assessed by up- and down-regulation of integrin α5 and β1 with RNA interference, as well as through ERK1/2 inhibition with U0126. ***Results:*** Osteogenesis of rBMSCs seeded on the Ta surface was superior to that of cells seeded on the Ti surface in terms of ALP activity, extracellular matrix calcification, and the expression of integrin α5, integrin β1, ERK1/2, Runt-related transcription factor 2, osteocalcin, collagen type I, and ALP at both the mRNA and protein levels. Moreover, down-regulation of integrin α5 or integrin β1, or ERK1/2 inhibition severely impaired the osteoblastic differentiation on the Ta surface. By contrast, over-expression

M. Lu and X. Zhuang contributed equally to this work.

Derong Zou and Huiliang Cao Department of Stomatology, Shanghai Jiao Tong University Affiliated Sixth People's Hospital, Shanghai 200233; State Key Laboratory of High performance Ceramics and Superfine Mictrostructure, Shanghai Institute of Ceramics, Chinese Academy of Sciences, Shanghai 200050 (China); E-Mail drzou@sjtu.edu.cn; hlc@mail.sic.ac.cn

of integrin α5 or integrin β1 improved osteogenesis on the Ti substrates, while subsequent ERK1/2 inhibition abrogated this effect. ***Conclusion:*** The integrin α5β1/ERK1/2 pathway plays a crucial role in regulating rBMSCs osteogenic differentiation; thus, the greater ability of a Ta surface to trigger integrin α5β1/ERK1/2 signaling may explain its better osteoinductivity. The different effects of Ta and Ti surfaces on rBMSC osteogenesis are considered to be related to the conductive behaviors between integrin α5β1 and the oxides spontaneously formed on the two metals. These results should facilitate the development of engineering strategies with Ta and Ti surfaces for improved osteogenesis in endosteal implants.

Introduction

Titanium (Ti) is a commonly used implant material for orthopedic and dental treatments owing to its good corrosion resistance and excellent biocompatibility [1]. Tantalum (Ta) also has outstanding corrosion resistance and biocompatibility, with great potential for extensive use in endosteal implants [2]; thus, the effect of Ti and Ta on osteogenesis has emerged as an important topic in the field of biomaterials science [3-5]. Several studies have demonstrated that Ta exhibits better osteoinductive and osseointegration capability than Ti in forms of bulk prosthesis, implant coatings, and bone tissue scaffolds [5-10]; however, the underlying mechanisms and intrinsic chemical differences between the two metals contributing to these effects on osteogenesis have not yet been verified.

Osteoinductivity and osseointegration are determined by both the structural and chemical characteristics of the material surface [11, 12]. However, most previous studies employed Ta and Ti samples on specific surface structures such as those with relatively high roughness (Ra = 0.29–0.37 μm) [3], nanostructure (nanotube of 100 nm in diameter and 300 nm in height) [13], and porous structure (pore size of 400–600 μm and porosity of approximately 80%) [14]. Since these structural properties will inevitably affect the osteoblastic differentiation of adherent cells [15-17], the osteoinductive performance associated with the inherent chemical properties of the two materials may be masked. Thus, use of a smooth surface could help to better reveal these differences, which would potentially eliminate these confounding effects [18-20].

Mesenchymal stromal cells (MSCs) from the bone marrow are multipotent stem cells that go through osteoblastic differentiation crucial for bone formation [21]. The interactions between MSCs and material surfaces generate important signals that mediate MSC behaviors, and such interactions largely involve integrins [22]. As transmembrane proteins composed of α and β subunits, integrins function as important cell receptors to the extracellular environment and are key components in the cell sensory system, thus playing a pivotal role during the adherence and spread of cells on material surfaces, ultimately determining the cell fate [22, 23]. To date, integrin α5β1 is one of the few integrins shown to participate in MSC osteogenesis [22]. Specifically, enhancing integrin α5 or β1 expression can initiate the differentiation of MSCs into osteoblasts [23], and inhibiting the two subunits interferes with this process [24]. Moreover, molecular analyses demonstrated that the integrin α5β1-induced osteoblast differentiation is mediated by activation of mitogen-activated protein kinases 3 and 1 (ERK1/2) signaling [23, 25]. Accordingly, we hypothesized that the intrinsic effects of Ta and Ti on cell osteogenesis can be uncovered by studying the integrin α5β1/ERK1/2-related activities in bone cells.

To test this hypothesis, in the present study, the adhesion and subsequent osteogenesis of rat bone mesenchymal stromal cells (rBMSCs) on polished Ta and Ti substrates were studied systematically. In addition, the up- and down-regulation of integrin α5 and β1 subunits as well as ERK1/2 inhibition were applied to assess the specific effect of the integrin α5β1/ERK1/2 pathway on Ta- and Ti-mediated osteogenesis. This study aims at improving our knowledge on the osteoinductive performance of the two material surfaces and the related molecular mechanisms.

Materials and Methods

Substrate preparation and characterization

Commercial pure Ti (thickness of 1 mm) and Ta (thickness of 0.5 mm) sheets were cut into 10-mm^2 or 20-mm^2 plates, and one side was polished to a mirror finish. The surface morphology of the fabricated plates was observed by scanning electron microscopy (SEM; S-3400, Hitachi, Japan), and the surface roughness was assessed by atomic force microscopy (AFM; ARTCAM-130, SII Nano Tech, Japan). The chemical states for Ta and Ti were determined by X-ray photoelectron spectroscopy (XPS; Axis Ultra, Kratos Analytical Ltd., Japan) using an aluminum target. The wettability was measured with 1 μL of distilled water (SL200B, Solo Tech Co Ltd., USA) at room temperature. To monitor the ion release kinetics of Ti and Ta, the plates were immersed in complete medium [CM; Dulbecco's modified Eagle medium (Gibco, USA) containing 10% fetal bovine serum (Gibco, USA), 100 U/mL penicillin, and 100 mg/L streptomycin] or osteogenic medium [OM; complete medium plus 50 M ascorbic acid (Sigma, USA), 10 mM β-glycerophosphate (Sigma, USA), and 100 nM dexamethasone (Sigma, USA)] and statically incubated at 37°C for 72 h. The ratio between the surface area (cm^2) of the samples and the volume of the medium (mL) was 1:1, and the resulting solutions were filtered by a microporous membrane before being subject to inductively coupled plasma optical emission spectrometry (ICP-OES; Vista AX, USA). This procedure was also applied to prepare Ta and Ti extracts as the culture medium for the cell osteogenesis assay; abbreviations of the culture media used in this study are listed in Table 1.

Cell isolation, identification, and culture

Cells from 12-week-old male Sprague-Dawley rats were used in this study. The animal experimental protocols were reviewed and approved by the Animal Care and Use Committee of Shanghai Jiao Tong University Affiliated Sixth People's Hospital (Approval Number: 2017-0269). The rBMSCs were isolated and cultured according to a previously reported method [26]. In brief, both of the femora were detached, the two ends were cut off at the epiphysis, and the marrow was immediately rinsed out using CM. The primary rBMSCs were then cultured in CM at 37°C in a humidified atmosphere of 5% CO_2. Non-adherent cells were removed by changing the medium after 48 h, and then the medium was replaced every 3 days thereafter. The cells were subcultured using trypsin/ethylenediaminetetraacetic acid (EDTA) (0.25% w/v trypsin, 0.02% EDTA) when 80–90% confluence was reached. Only rBMSCs at passage 3–5 were used for further study.

The rBMSCs were identified by an immunofluorescence assay. The cultured cells were positively immunostained with CD44, CD90, and CD105, and negatively stained with CD45 and CD34 (Fig. S1 - For all supplemental material see www.karger.com/ 10.1159/000495280/), which met the minimal criteria to define BMSCs according to the Mesenchymal and Tissue Stem Cell Committee of the International Society for Cell Therapy [27].

To evaluate the effect of Ta and Ti samples on cell behavior, culture plastic (Cp) was shaped to the same size of the samples and used as a control. All of the substrates were sterilized with 75% alcohol for 3 h and rinsed twice with sterile phosphate buffer saline (PBS) before cell seeding. Both OM and CM were replaced every 3 days after the rBMSCs were added to the substrates.

Cell adhesion and spreading assays

To assess the effects of polished Ta and Ti substrates on the early adhesion and spread of rBMSCs, cells (1×10^4 cells/well) were seeded on Ta, Ti, and Cp substrates (1 cm^2) in 24-well plates and cultured in CM for 24 h. The cells were then washed with PBS and fixed in a 4% formaldehyde solution for 10 min. After cell membranes were permeated by 0.1% Triton X-100 (Sigma, USA) for 3 min, TRITC-phalloidin (Yeasen, China) and 4, 6-diamidino-2-phenylindole (DAPI; Beyotime, China) were co-incubated with the cells at 37°C in the dark for 40 min and 5 min, respectively.

Table 1. Abbreviations of the culture media used in this study

Abbreviation	Culture medium
OM	Osteogenic medium
CM	Complete medium
Ta/OM	Ta extract from osteogenic medium
Ta/CM	Ta extract from complete medium
Ti/OM	Ti extract from osteogenic medium
Ti/CM	Ti extract from complete medium

The cell morphology on different substrates was observed by fluorescence microscopy (IX 70, Olympus, Japan), and 10 images of substrates of each type were obtained. The calculation of cell spreading area was carried out by image analysis with Image-Pro Plus 6.0 software.

Cell proliferation assay

The rBMSCs (1×10^4 cells/well) were seeded on the substrates (1 cm^2) in 24-well plates, and cultured in CM for 1, 3, 5, and 7 days. Cell proliferation was assessed with the CCK-8 assay (Dojindo, Kumamato, Japan) according to the manufacturer instructions. In brief, 1 mL of mixed solution (alpha-minimal essential medium and CCK-8 solution at a 10:1 ratio) was applied to each well and incubated at 37°C for 4 h. Then, 100 μL of the suspension was introduced to a 96-well plate, and the optical density (OD) was read at 450 nm (Thermo, USA).

Alkaline phosphatase (ALP) activity assay

The osteoinductive effect of Ta and Ti surfaces was evaluated by an ALP activity assay. The rBMSCs (1×10^4 cells/well) were cultured on the substrates (1 cm^2) in 24-well plates in OM and CM. At day 7 and 14, the ALP activity was measured with an ALP activity kit (Nanjing Jiancheng Bioengineering Institute, China). In brief, the substrates were rinsed with cold PBS three times and transferred to new plates. Cells on the substrates were lysed by RIPA (Beyotime, China) on ice, the lysates were reacted with a working solution at 37°C for 15 min, and the OD values of the resulting solution were measured at 520 nm (Thermo, USA). Finally, ALP levels were normalized to the total intracellular protein content determined using the bicinchoninic acid protein assay (Beyotime, China). To further determine whether the Ta and Ti substrates exerted an osteoinductive effect by releasing ions into the culture medium, the ALP activity of rBMSCs cultured in OM, CM, Ta/OM, Ti/OM, Ta/CM, and Ti/CM for 7 days was determined and compared using the same ALP activity kit.

Furthermore, an ALP staining kit (Beyotime, China) was used to evaluate ALP activity and expression. In brief, BCIP/NBT working solution was added to each well containing a cell-attached substrate and incubated in the dark at room temperature for 30 min after cell fixation with a 4% formaldehyde solution for 10 min. The substrates were rinsed with distilled water for microscopic observation (IX 70, Olympus, Japan).

Osteocalcin (OCN) and collagen-I (COL-I) secretion assays

To further investigate the intermediate- and long-term influence of Ta and Ti surfaces on rBMSC osteogenesis, the cells (1×10^4 cells/well) were added onto the different substrates (1 cm^2) and cultured in 24-well plates in OM and CM. After 7 and 14 days, the concentrations of cell-secreted OCN and COL-I in the medium supernatants were measured by a rat OCN enzyme-linked immunoassay (ELISA) kit (Bio-swamp, China) and a rat COL-I ELISA kit (Bio-swamp, China), respectively. The standards for each assay were prepared at a series of concentrations and run in parallel with the samples. The OD was read at 450 nm using a microplate reader (Thermo, USA), and the levels of OCN and COL-I (ng/mL) were calculated in reference to the corresponding standard curves.

Extracellular matrix (ECM) calcium deposition assay

Calcium deposition in the ECM was evaluated by an Alizarin Red staining assay to identify the final effects of the Ta and Ti surfaces on the osteoblastic differentiation of rBMSCs. Cells (5×10^3 cells/well) were seeded on the substrates (1 cm^2) in 24-well plates and cultured in OM. After 14 and 21 days, the samples were washed three times in PBS and transferred to new plates. The adherent cells were fixed in 0.5 mL of 75% ethanol for 1 h, and then the substrates were stained with 40 mM Alizarin Red (Solarbio, China) for 10 min. Unbound red residue was rinsed with PBS, and images of different substrates were captured by optical microscopy. The bound stain was eluted using 10% cetylpyridinium chloride (Sigma, USA) in 10 mM sodium phosphate, and the OD values of the resulting solution were measured at 600 nm (Thermo, USA).

Integrin α5 and β1 immunofluorescence staining assay

The rBMSCs (5×10^4 cells/well) were seeded on the different substrates (1 cm^2) in 24-well plates and cultured in OM and CM for 24 h. Attached cells were fixed in 4% paraformaldehyde for 30 min and permeabilized with 0.1% Triton X-100 for 20 min. After washing with PBS, the cells were incubated for 1 h

at room temperature in blocking solution (1% bovine serum albumin in PBS), and then treated with integrin α5 (1:250, Santa Cruz Biotechnology, Santa Cruz, CA, USA, sc-376199,) and integrin β1 (1:100, Santa Cruz Biotechnology, Santa Cruz, CA, USA, sc-9970) primary antibodies at 4°C overnight. Subsequently, the cells were incubated with the secondary antibody (1:400, Beyotime, China, A0428) for 1 h and with DAPI for 5 min. Images were obtained by fluorescence microscopy (IX 70, Olympus, Japan).

Osteogenic gene expression assay

The rBMSCs were added to the different substrates (4 cm^2) in 6-well plates and cultured in OM and CM. The mRNA expression levels of integrin α5, integrin β1, Runt-related transcription factor 2 (*Runx2*), *Alp*, *Ocn*, and *Col-I* were measured by real-time reverse-transcriptase polymerase chain reaction (RT-PCR) at day 1 (5×10^5 cells/well), 7 (1×10^5 cells/well), and 14 (5×10^4 cells/well). First, the substrates were washed with PBS and transferred to new wells, and the RNA was extracted using TRIzol reagent (Invitrogen, USA) to obtain the cell lysate. Proteins separation was performed using chloroform, and RNA was recovered using isopropanol and precipitated by alcohol. The complementary first-strand DNA (cDNA) was synthesized from total RNA using the PrimeScript RT reagent kit (Takara, Japan). In brief, the single-stranded cDNA was synthesized by incubating 25 μL of the complete reaction mixture (RNA-Primer Mix, 5× RT Reaction Buffer, 25 mM dNTPs, 25 U/μL DNase Inhibitor, 200 U/μL M-MLV Rtase, oligo $(dt)_{18}$, and RNase-free ddH_2O) for 60 min at 37°C, followed by incubation at 85°C for 5 min and 4°C for 5 min. Real-time PCR was conducted on the Bio-Rad C1000 system using SYBR Premix Ex Taq (Takara, Japan) to amplify and quantify the target cDNA. The PCR mixture (SYBR Premix Ex TaqII, primer, cDNA solution and ddH_2O) was prepared in a final volume of 25 μL, and subjected to 40 cycles of denaturation, annealing, and extension for all genes using the primers listed in Table 2. The expression level of the housekeeping gene *Gapdh* was used to normalize that of the target genes.

Osteogenic protein expression assay

The rBMSCs were added to the different substrates (4 cm^2) in 6-well plates and cultured in OM and CM. The protein expression levels of integrin α5, integrin β1, RUNX2, ALP, phosphorylated (p)-ERK1/2, and total (T)-ERK1/2 were measured by western blotting (WB) at day 1 (5×10^5 cells/well), 7 (1×10^5 cells/well), and 14 (5×10^4 cells/well). Total protein extraction was performed with RIPA lysis buffer and then centrifuged at 12, 000 ×*g* for 20 min at 4°C. Proteins in the cell lysates were separated by 10% sodium dodecyl sulfate-polyacrylamide gel electrophoresis and transferred to a polyvinylidene fluoride membrane (Bio-Rad, USA). Blots were blocked by incubating with skim milk for 1 h, followed by incubation with integrin α5 (1:2000, Abcam, UK, ab150361), integrin β1 (1:10000, Abcam, UK, ab183666), p-ERK1/2 (1:5000, Abcam, UK, ab50011), ERK1/2 (1:1000, Abcam, UK, ab17942), RUNX-2 (1:1000, Abcam, UK, ab23981), ALP (1:3000, PL Laboratories Inc., Canada, PL0502328), or GAPDH (1:2000, Cell Signaling Technology, USA, 5174) primary antibodies at 4°C overnight. Finally, the membranes were incubated with peroxidase-conjugated secondary antibodies (1:1000, Beyotime Biotechnology, China, A0208, A0181, and A0216) for 2 h at room temperature, and the blots were analyzed using an enhanced chemiluminescence detection kit (Pierce, USA).

Table 2. Primers used for real-time RT-PCR

Gene	Sequences (F, forward; R, reverse)
integrin α5-forward	5′-ACGGCTACAATGATGTCG-3′
integrin α5-reverse	5′-GGAAGGCTTAGTGTTCAGTC-3′
integrin β1-forward	5′-ATGATGCGTGCGGAAGAC-3′
integrin β1-reverse	5′-GAAGGCGTTGGGAGTTACAG-3′
ERK1-forward	5′-TCTGCCCTACTCATCCTG-3′
ERK1-reverse	5′-GCCTCCACATCCAATCAC-3′
ERK2-forward	5′-AATAAGGTGCCGTGGAAC-3′
ERK2-reverse	5′-TTCAGCAATGGGCTCATC-3′
RUNX-2-forward	5′-ACTTCGTCAGCGTCCTATC-3′
RUNX-2-reverse	5′-CATCAGCGTCAACACCATC-3′
ALP-forward	5′-AAGCACTCCCACTATGTC-3′
ALP-reverse	5′-GTCAGGTTGTTCCGATTC-3′
OCN-forward	5′-GGGCAGTAAGGTGGTGAATAG-3′
OCN-reverse	5′-AGTCCTGGAGAGTAGCCAAAG-3′
COL1-forward	5′-TGAAGTCCTCTCCTCCCTACC-3′
COL1-reverse	5′-CTGCGTCACAGCGTATTCC 3′
GAPDH-forward	5′-GGAGTCTACTGGCGTCTTCAC-3′
GAPDH-reverse	5′-ATGAGCCCTTCCACGATGC-3′

Cell transfection and inhibitor treatment

Fig. S2 provides a schematic overview of the approach used to verify the role of the integrin α5β1/ERK1/2 pathway in the regulatory mechanism of rBMSC osteogenesis on Ta and Ti surfaces. The following specific integrin α5 and integrin β1 small hairpin RNA (shRNA) sequences (Sangon Biotech Co., Ltd., China) were cloned into the pLKO.1-puro lentiviral vector (Addgene, USA): integrin α5-shRNA (nucleotides 1233–1255), 5'-GCAGGGTCTACATCTATCT-3'; integrin β1-shRNA (nucleotides 1651–1673), 5'-ATTCTGCGAGTGTGATAAC-3'. The specific coding sequences of rat integrin α5 or integrin β1 were cloned into the pCDNA3.1(+) vector (Addgene, USA) with the following primers: integrin α5-F 5'-CCCAAGCTTATGCCCCCCCGCCAGCCGA-3', integrin α5-R 5'-CCGGAATTCGGCATCTGAGGTGGCTGGAG-3'; integrin β1-F 5'-CCCAAGCTTATGAATTTGCAACTGGTTTT-3', integrin β1-R 5'-CCGGAATTCTTTTCCCTCATACTTCGGAT-3'. To silence integrin α5 or integrin β1 expression, rBMSCs (3×10^5 cells/well) were transfected with 1.5 μL of pLKO.1-puro-integrin α5-shRNA, pLKO.1-puro-integrin β1-shRNA, or blank pLKO.1-puro lentiviral vector as the negative control (NC) in 6-well plates, and incubated for 6 h. For the over-expression of integrin α5 or integrin β1, the cells (3×10^5 cells/well) were transduced with blank pCDNA3.1(+) vector as the NC, pCDNA3.1(+)-integrin α5 or pCDNA3.1(+)-integrin β1 in 6-well plates, and incubated for 6 h. The transfection efficiency was identified by real-time RT-PCR and WB assays.

The rBMSCs with down-regulated integrin α5 or integrin β1 expression were added to Ta substrates (4 cm^2) in 6-well plates and cultured in CM. In addition, untransfected cells were also seeded on Ta substrates and treated with 1 μM ERK1/2 inhibitor (U0126) (Selleck, China) for 24 h. The cells with integrin α5 or integrin β1 over-expression were incubated on the Ti substrates (4 cm^2) in the absence or presence of U0126 treatment. The gene and protein expression levels of integrin α5, integrin β1, RUNX2, ALP, and ERK1/2, as well as ALP activity were examined at day 1 (5×10^5 cells/well) and 7 (1×10^5 cells/well).

Statistical analysis

All data are expressed as mean ± standard deviation from at least three independent experiments, and were analyzed by one-way ANOVA combined with Tukey's post-hoc test using GraphPad Prism software version 5.0; $p < 0.05$ was considered statistically significant.

Results

Surface features of polished Ta and Ti substrates

Fig. 1A and B show typical SEM images of the Ti and Ta surfaces, demonstrating that both substrates were smooth at the nano-scale. The average surface roughness (Ra) determined by AFM did not differ between the Ti and Ta substrates (Fig. 1C, D). The water contact angles were lower on the Ti substrates ($p < 0.05$) (Fig. 1E, F), indicating that the Ta surface is slightly more hydrophobic. Moreover, judging from the binding energies of Ti and Ta determined by XPS, both the Ti and Ta surfaces were spontaneously oxidized during exposure to the atmosphere. The Ti 2p doublets at 457.89 eV/463.39 eV (acquired from the surface of the Ti substrate, Fig. 2A) and 458.89 eV/464.29 eV (acquired from a 5 nm depth of the Ti substrate, Fig. 2C) could be assigned to TiO_2, and the doublets at 455.30 eV/460.80 eV and 456.92 eV/461.92 eV (Fig. 2C) likely correspond to TiO and Ti_2O_3, respectively, based on the NIST X-ray Photoelectron Spectroscopy Database (https://srdata.nist.gov/xps/). In addition, the Ta 4f doublets at 25.880 eV/27.765 eV (acquired from the surface of the Ta substrate, Fig. 2B) and 26.480 eV/28.441 eV (acquired from a 5 nm depth of the Ta substrate, Fig. 2D) could be assigned to Ta_2O_5, and the doublets at 20.591 eV/22.369 eV (Fig. 2B) and 22.150 eV/24.040 eV (Fig. 2D) correspond to metallic Ta based on the NIST X-ray Photoelectron Spectroscopy Database (https://srdata.nist.gov/xps/). In addition, the amount of Ti and Ta released by the corresponding substrates was negligible (<0.002 μg/mL for Ti and <0.01 μg/mL for Ta, which were all below the detectable limit of ICP-OES).

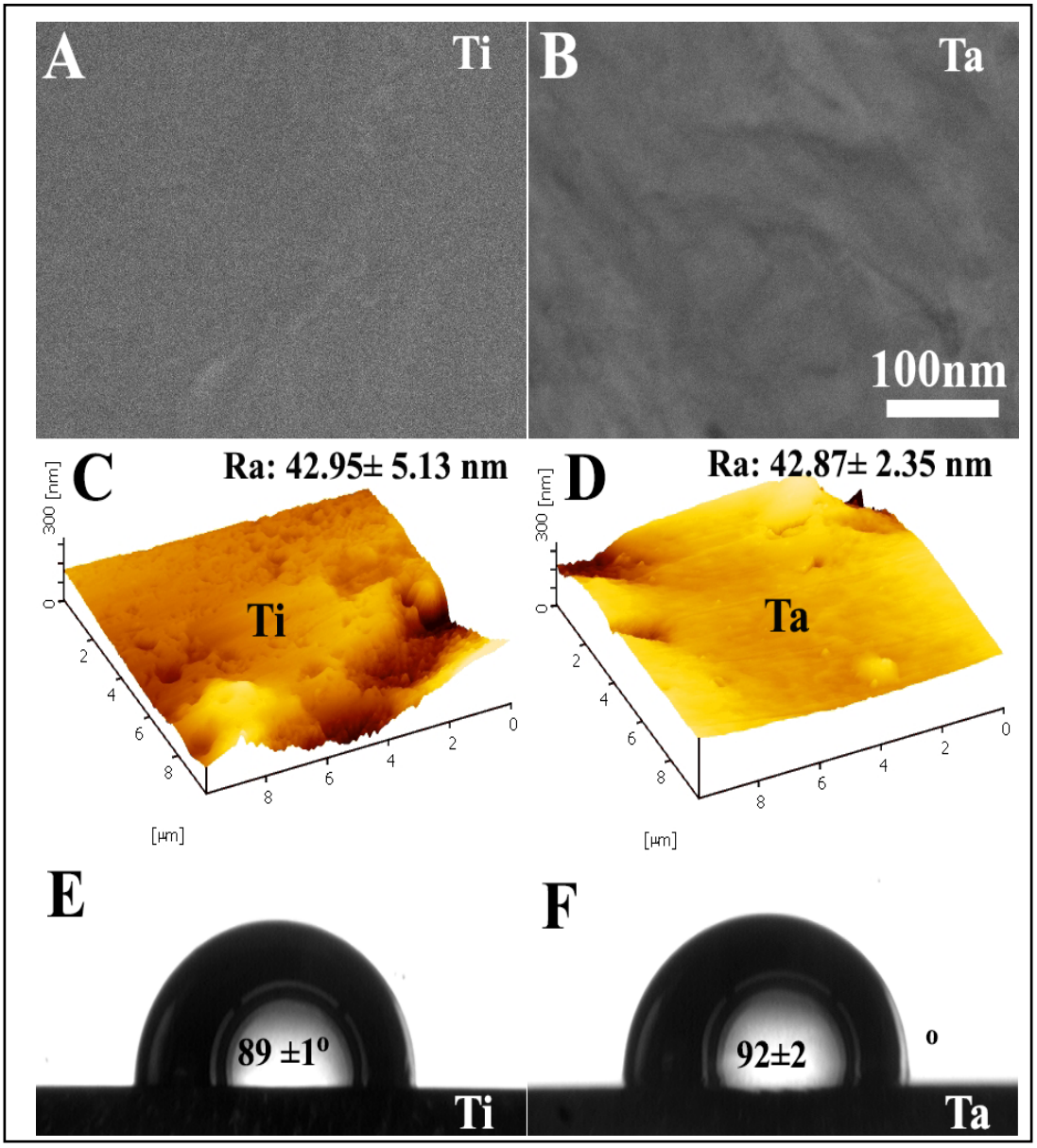

Fig. 1. Surface characterization of Ti and Ta substrates. SEM observations of the morphology of the (A) Ti surface and (B) Ta surface; AFM image of the (C) Ti surface and (D) Ta surface; water contact angle on the (E) Ti surface and (F) Ta surface.

Effects of Ta and Ti surfaces on rBMSC adhesion and proliferation

As shown in Fig. 3A, the morphology of the rBMSCs on the Ta, Ti, and Cp surfaces was similar at each time point. Furthermore, the average spreading areas on the Ta, Ti, and Cp substrates did not differ significantly among the three substrates at each time point (Fig. 3B). The cell proliferation rate was also similar on the Ta and Ti surfaces (Fig. S3).

ALP activity, OCN, and COL-I secretion

There was no discernable difference in the ALP activity of rBMSCs in OM, Ta/OM, and Ti/OM, or among groups cultured with CM, Ta/CM, and Ti/CM (Fig. 3C).

However, the rBMSCs seeded on the Ta surface displayed the highest ALP activity overall (Fig. 4A, C). In addition, the ALP activity on the Cp substrates was lower than that on the Ti substrates in both OM and CM at each time point, although the difference observed in the

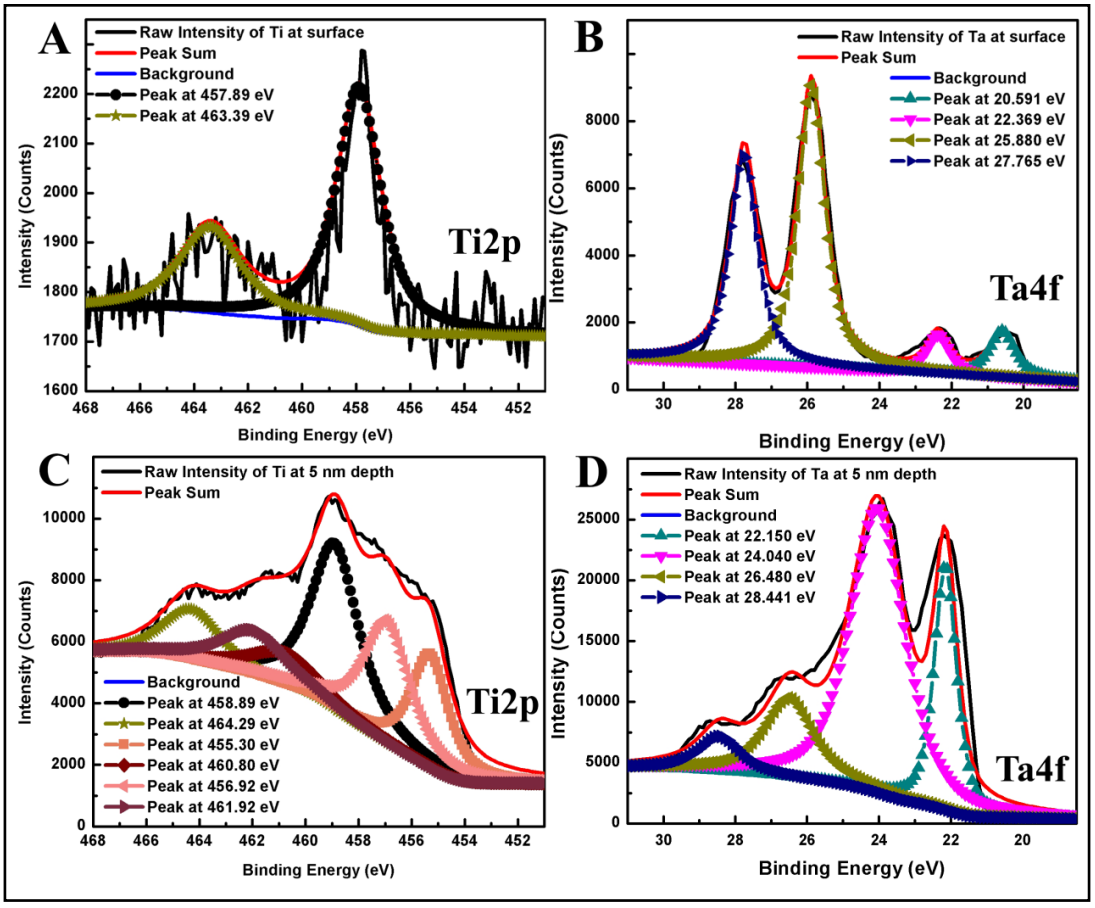

Fig. 2. Chemical states of Ti and Ta on the samples. XPS spectra of the (A) surface and (C) 5 nm depth on the Ti substrate, and of the (B) surface and (D) 5 nm depth on the Ta substrate.

OM at day 14 did not reach statistical significance. These results were supported by the ALP staining assay (Fig. 4B, D).

The secretion of OCN and COL-I on the Ta surface was significantly higher than that on the Ti and Cp surfaces in both media at day 7 and 14 (Fig. S4A, B). However, the cells on the Ti surface secreted more OCN than those on the Cp surface in OM at day 7, although there was no significant difference in OCN and COL-I secretion between cells on the Ti and Cp surface in each medium at any time point.

Calcium nodules in the ECM on Ta and Ti surfaces

As shown in Fig. 4E, the amount of calcium nodules in the ECM on the Ta substrate was greater than that on the other two substrates at day 14 and 21, whereas there was no difference between the Ti and Cp substrates detected at any time point. Light microscopy images of Alizarin Red staining confirmed these findings (Fig. 4F).

Effect of Ta and Ti surfaces on expression of the integrin α5β1/ERK1/2 pathway in rBMSCs

The mRNA expression levels of integrin α5, integrin β1, *Runx2*, and the downstream effectors *Alp*, *Ocn*, and *Col-I* in rBMSCs on the Ta surface increased by 1.5–2.1-fold compared to those on the Ti surface in both media at all time points (Fig. 5A–D; Fig. S4C, D). By contrast, the cells on the Ti surface displayed higher mRNA expression levels of integrin α5, integrin β1, and *Alp* in both media at day 1, 7, and 14, and of *Runx2* at days 1 and 7 (approximately 1.2–1.6 fold) when compared with those of cells on the Cp surface (Fig. 5A–D). However, greater mRNA expression levels of *Ocn* and *Col-I* were only detected on the Ti surface (approximately

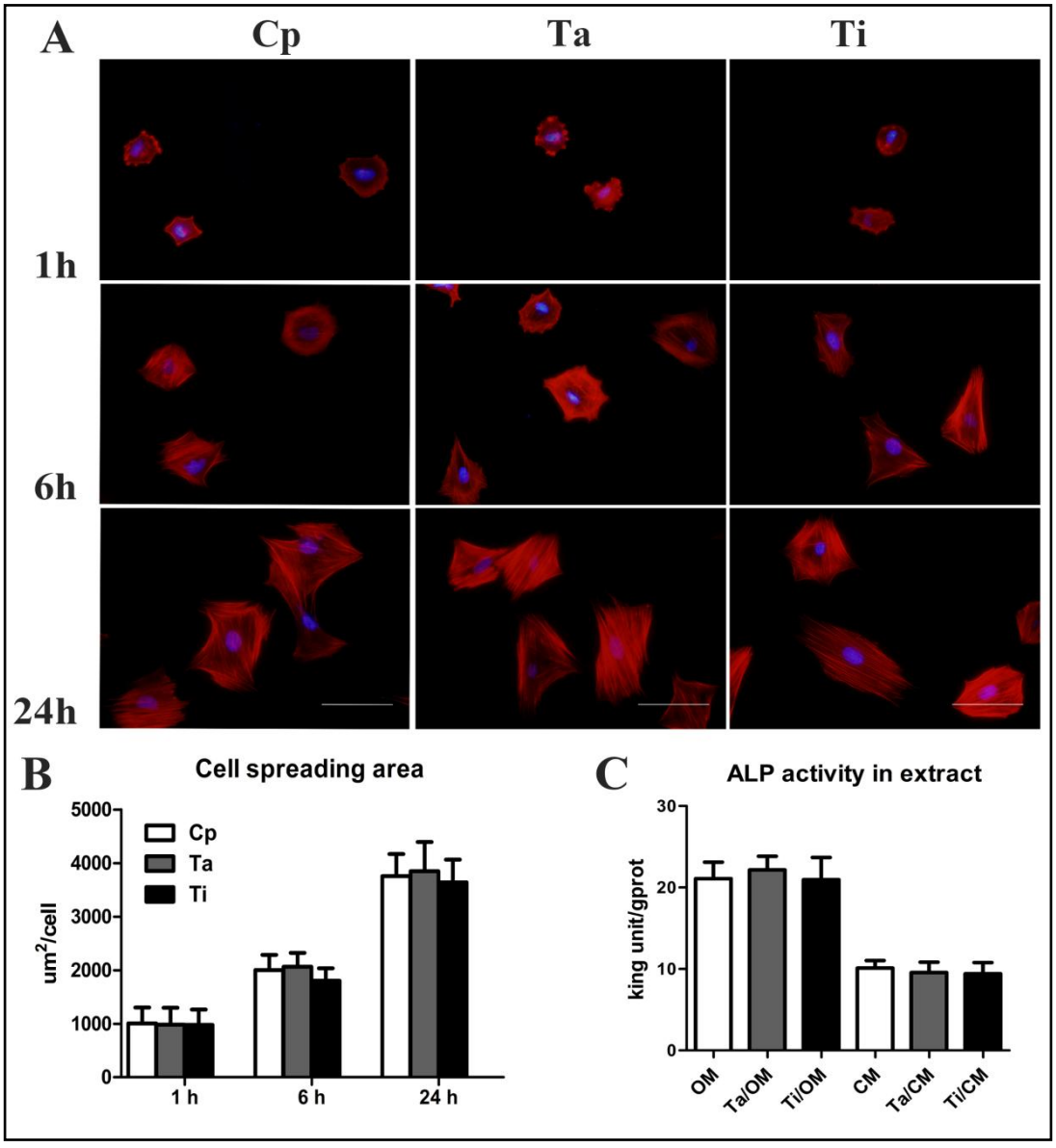

Fig. 3. Morphology of rBMSCs on different substrates and ALP activity in corresponding medium extracts. (A) Morphology of cells attached on Ta, Ti, and Cp surfaces at 1, 6, and 24 h; actin filaments were stained with phalloidin (red) and nuclei were stained with DAPI (blue). Scale bar: 100 μm. (B) Average spreading area of attached cells; comparisons were conducted between samples at the same time point. (C) Cell ALP activity in OM, CM, Ta/OM, Ti/OM, Ta/CM, Ti/CM at day 7; comparisons were conducted between samples in corresponding medium extracts.

1.2-fold) in OM at day 7 and in CM at day 14 in comparison to those of cells on the Cp surface (Fig. S4C, D).

The WB analysis clearly indicated that the protein expression of integrin α5, integrin β1, RUNX-2, and ALP, as well as ERK1/2 phosphorylation was elevated (approximately 1.2–1.6 fold) on the Ta surface in comparison to that on the Ti surface in both media at days 1, 7, and 14 (Fig. 5E–H; Fig. S5). Moreover, the immunofluorescent assay revealed more pronounced protein expression of integrin α5 and integrin β1 on the Ta substrates than on the Ti substrates in both media at day 1 (Fig. 6A, B). In addition, the cells on the Ti surface demonstrated higher protein expression levels of integrin α5, integrin β1, and ALP (approximately 1.2–2 fold) in both media at days 1, 7, and 14 when compared with those

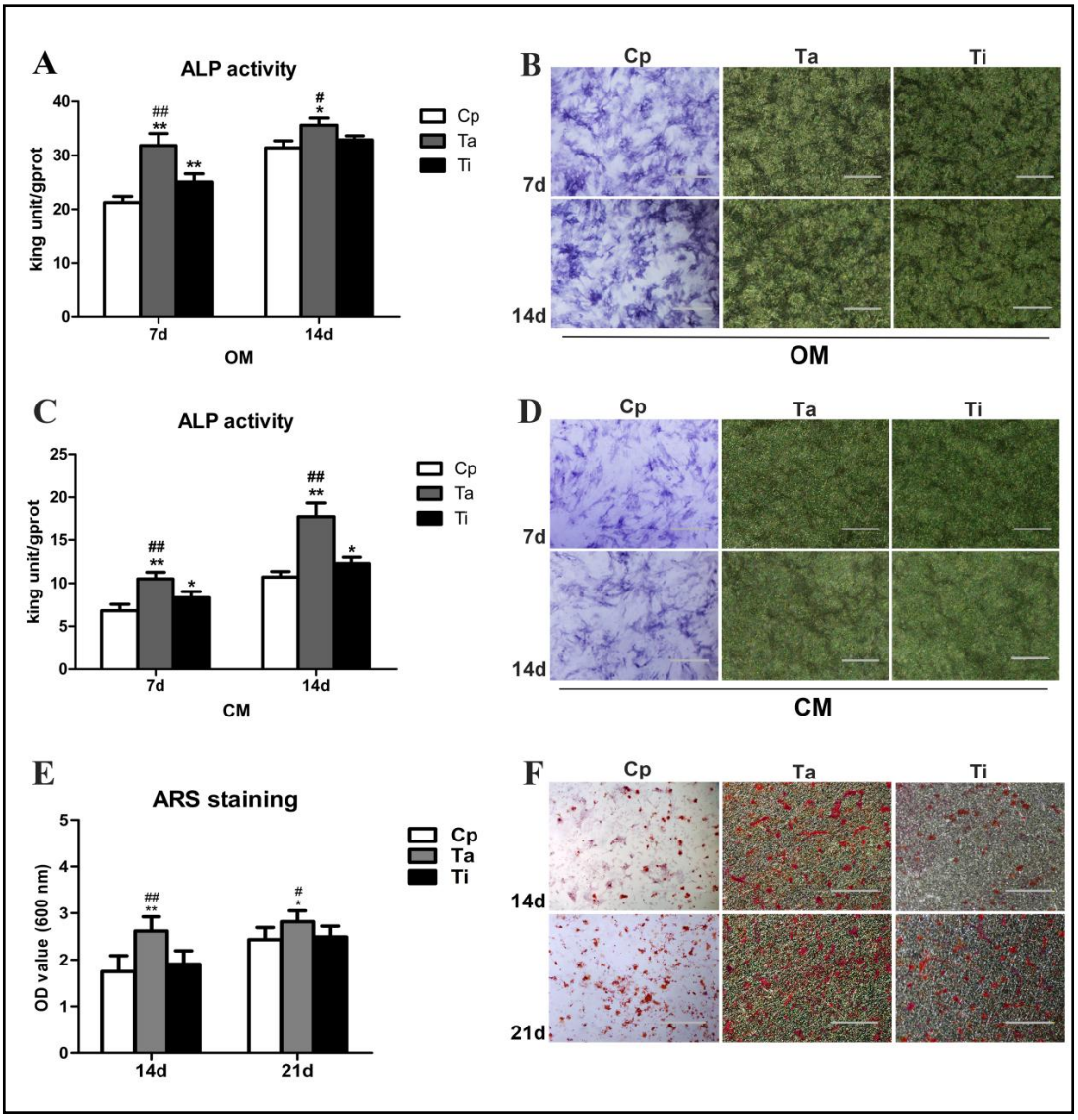

Fig. 4. Osteogenic differentiation of rBMSCs on Ta, Ti, and Cp surfaces. ALP activity of cells cultured in (A) OM and (C) CM for 7 and 14 days; corresponding ALP staining in (B) OM and (D) CM. Scale bar: 500 μm. (E) Quantification and (F) images of Alizarin Red staining at day 14 and 21. Scale bar: 2 mm; comparisons were conducted between samples at the same time point. *p<0.05, **p<0.01 compared with Cp; #p<0.05, ##p<0.01 compared with Ti.

on the Cp surface (Fig. 5E–G; Fig. S5A-C, E–G). Interestingly, RUNX2 was more intensively expressed on the Ti surface (about 1.7–2 fold) within a short incubation time (days 1 and 7) in both media compared to that detected on the Cp surface (Fig. 5E, G; Fig. S5A, C), whereas no such difference was detected at day 14 (Fig. S5E, G).

Integrin α5β1/ERK1/2 signaling interference suppressed the osteogenesis-promoting effect of the Ta surface

After transfection with integrin α5- or integrin β1-shRNA, rBMSCs exhibited a 75% and 70% reduction of integrin α5 and integrin β1 mRNA expression when compared with that of wild-type rBMSCs (control) or cells treated with a blank vector (NC). The transfection efficiency was further verified by a decrease of 75% in integrin α5 and of 70% in integrin β1 expression at the protein level. No significant difference was identified in the mRNA and

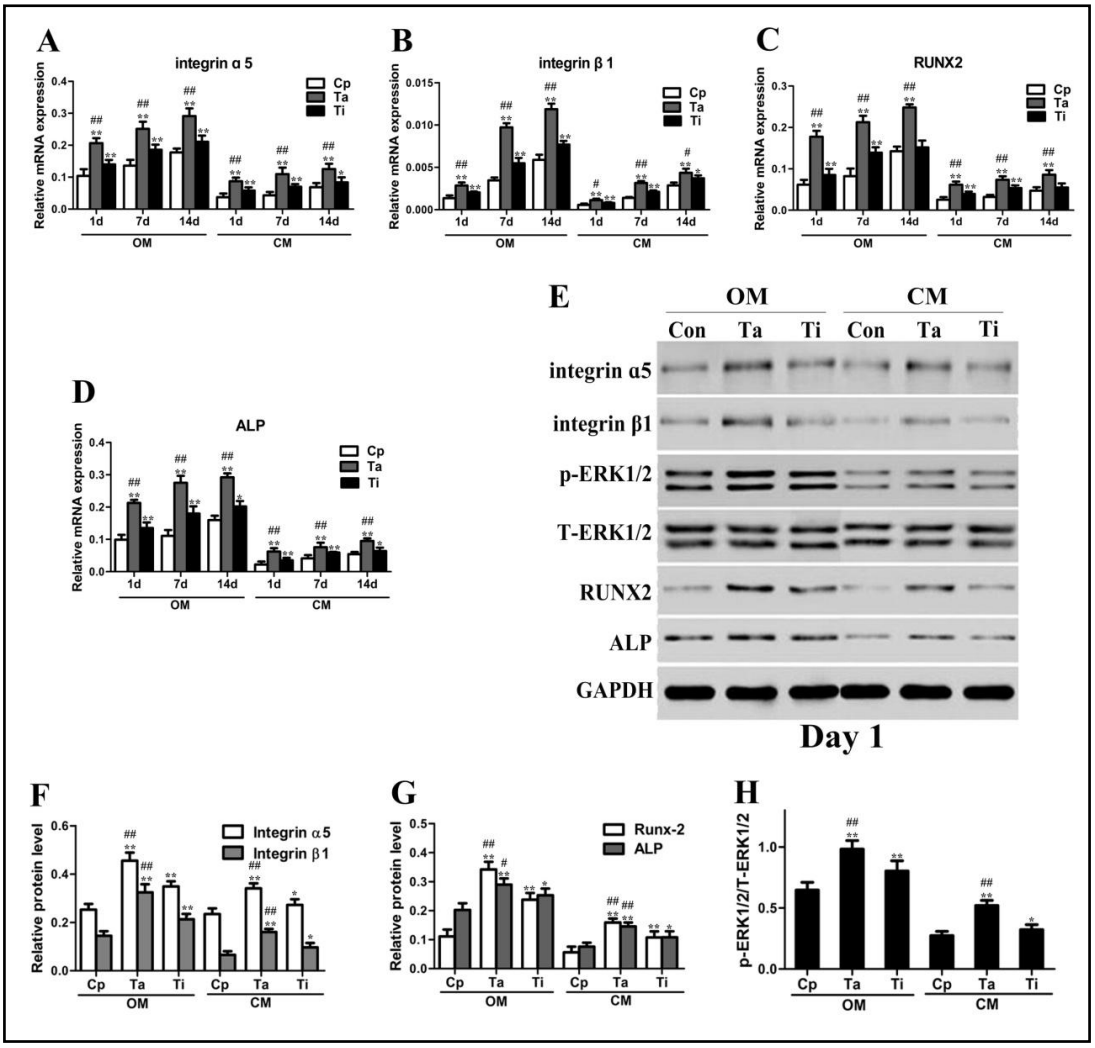

Fig. 5. Osteogenic phenotype of rBMSCs on Ta, Ti, and Cp substrates. mRNA expression levels of (A) integrin α5, (B) integrin β1, (C) Runx2, and (D) Alp in OM and CM at day 1, 7, and 14; the expression level of Gapdh was used to normalize that of target genes, and comparisons were conducted between substrates in the same medium at the same time point. (E) Osteogenic protein expression in OM and CM at day 1. The gray value of (F) integrin α5, integrin β1, (G) RUNX2, and ALP was normalized to that of GAPDH, and the grey value of (H) p-ERK was normalized to that of T-ERK1/2; comparisons were conducted between samples in the same medium. *p<0.05, **p<0.01 compared with Cp; #p<0.05, ##p<0.01 compared with Ti.

protein expression levels between the NC and control groups for the two target genes (Fig. S6A).

When compared with NC, the down-regulation of integrin α5 obviously reduced the expression of integrin β1 in rBMSCs on the Ta surface at day 1 (about a 65% decrease at the gene level and a 55% decrease at the protein level) and vice versa (Fig. 7A, B, G, H). Silencing of integrin α5 or integrin β1 expression significantly reduced the gene expression levels of *Erk1*, *Erk2*, *Runx2*, and *Alp* on the Ta surface (70–80% decrease; Fig. 7C–F), which was in line with the 50% decrease in ERK1/2 phosphorylation and 60% decrease in the protein expression of RUNX2 and ALP (Fig. 7G, I, J). In addition, treatment with the ERK1/2 inhibitor markedly reduced the expression levels of the downstream effectors RUNX2 and ALP, and the upstream mediators integrin α5 and integrin β1 (a 60–80% decrease at the gene level and a 50–60% decrease at the protein level; Fig. 7A, B, E, F, G–I). More importantly, knockdown of integrin α5 or integrin β1 expression as well as inhibition of ERK1/2 greatly

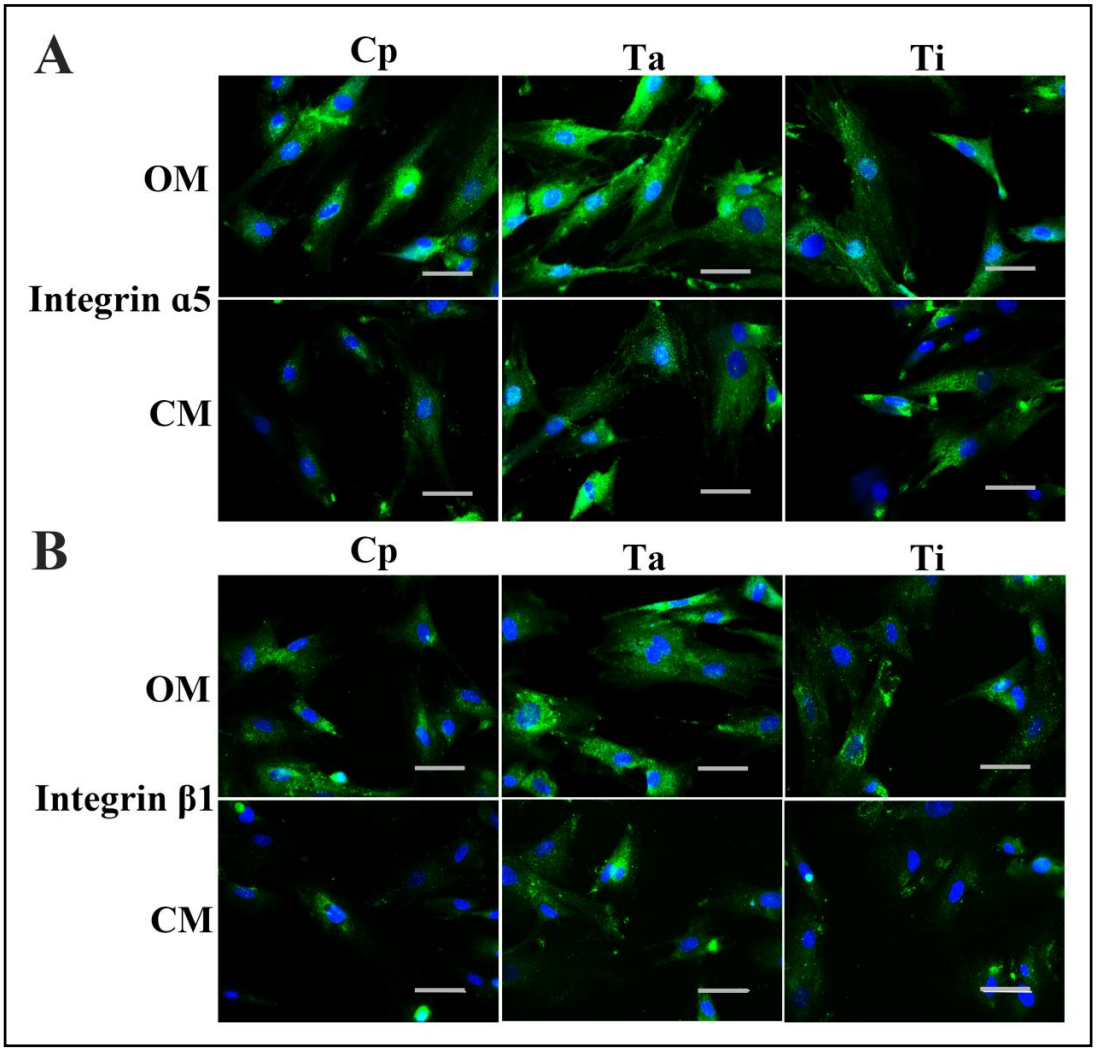

Fig. 6. Protein expression of integrin α5 and integrin β1 in rBMSCs on Ta, Ti, and Cp substrates. Immunostaining of (A) integrin α5 and (B) integrin β1 in OM and CM at 24 h; cell nuclei were stained with DAPI (blue). Scale bar: 50 μm.

reduced both the mRNA and protein expression levels of RUNX2 and ALP in rBMSCs on the Ta surface, reaching a similar or even lower level than those detected in the NC group on the Ti surface and in the wild-type cells on the Cp surface (control) (Fig. 7E, F, G, I).

rBMSCs with suppressed integrin α5β1/ERK1/2 signaling maintained lower gene and protein expression levels of RUNX2 and ALP in comparison to the NC on the Ta surface by day 7 (Fig. 7E, F; Fig. S7A, C). Furthermore, the interaction among integrin α5, integrin β1, and ERK1/2 caused by the knockdown of integrin α5 or integrin β1, or ERK1/2 inhibition, was quite similar to that detected at day 1 (Fig. 7A–D; Fig. S7A, B, D).

The reduced ALP expression on the Ta surface induced by down-regulation of the integrin α5β1/ERK1/2 pathway was confirmed by a 30% decrease in ALP activity at the corresponding time points (Fig. 7K).

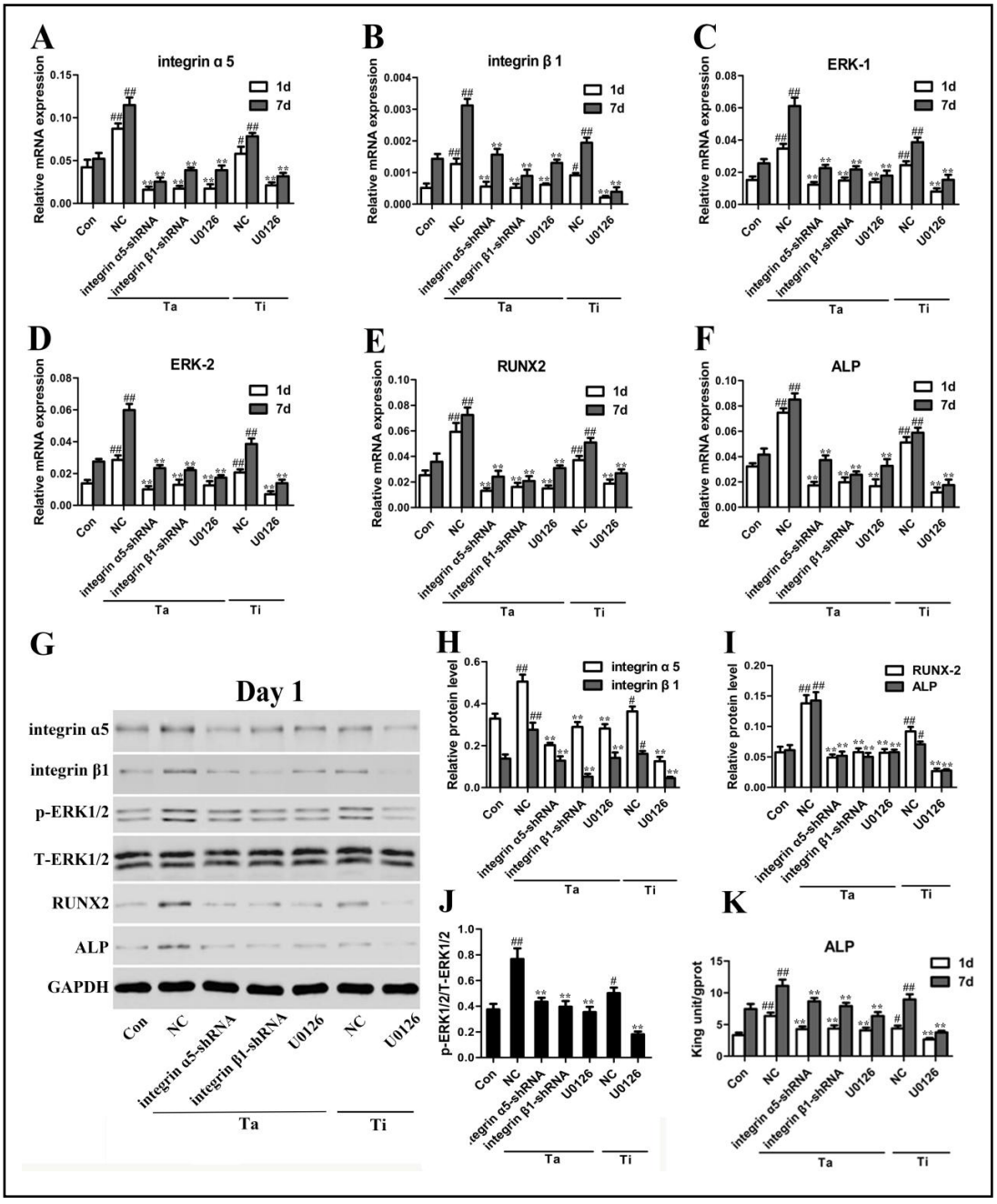

Fig. 7. Osteogenic phenotype of rBMSCs on the Ta substrate following down-regulation of the integrin α5β1/ERK1/2 pathway. mRNA expression levels of (A) integrin α5, (B) integrin β1, (C) Erk1, (D) Erk2, (E) Runx2, and (F) Alp in cells treated with blank vector (NC), integrin α5-shRNA, integrin β1-shRNA, or an ERK1/2 inhibitor (U0126) on the Ta surface, and those treated with NC or U0126 on the Ti surface in CM at day 1 and 7; the expression level of Gapdh was used to normalize that of the target genes, and comparisons were conducted between samples at the same time point. (G) Osteogenic protein expression in CM at day 1. The gray value of (H) integrin 5, integrin β1, (I) RUNX2, and ALP was normalized to that of GAPDH, and the grey value of (J) p-ERK was normalized to that of T-ERK1/2. (K) Corresponding ALP activity measured at day 1 and 7; comparisons were conducted between samples at the same time point. **p<0.01 compared with NC on the same substrate; #p<0.05, ##p<0.01 compared with the control (wild-type on the Cp substrate).

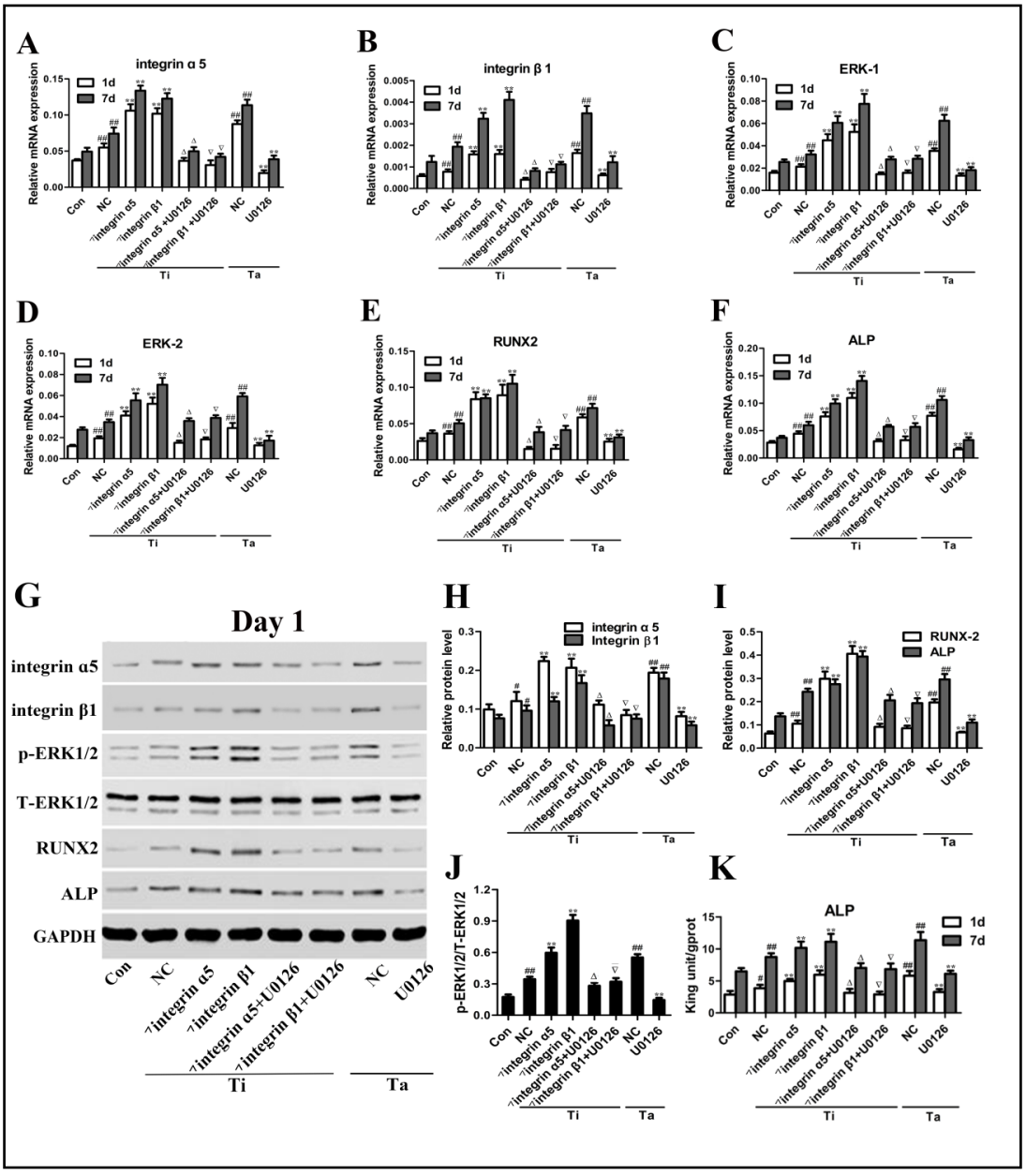

Fig. 8. Osteogenic phenotype of rBMSCs on the Ti substrate following up- and down-regulation of the integrin α5β1/ERK1/2 pathway. mRNA expression levels of (A) integrin α5, (B) integrin β1, (C) Erk1, (D) Erk2, (E) Runx2, and (F) Alp in cells treated with the blank vector (NC), integrin α5-coding sequence (^integrin α5), or integrin β1-coding sequence (^integrin β1) followed by treatment with the ERK1/2 inhibitor (U0126) or not on the Ti surface, and those treated with NC or U0126 on the Ta surface in CM at day 1 and 7. The expression level of Gapdh was used to normalize that of the target genes, and comparisons were conducted between samples at the same time point. Osteogenic protein expression in CM at day 1; the gray value of (H) integrin α5, integrin β1, (I) RUNX2, and ALP was normalized to that of GAPDH, and the grey value of (J) p-ERK was normalized to that of T-ERK1/2. (K) Corresponding ALP activity was measured at day 1 and 7, and comparisons were conducted between samples at the same time point. **p<0.01 compared with NC on the same substrate; #p<0.05, ##p<0.01 compared with the control (wild-type on the Cp substrate); △p<0.01 compared with ^integrin α5; ▽p<0.01 compared with ^integrin β1.

Effect of integrin α5β1/ERK1/2 signaling interference on rBMSC osteogenesis on the Ti surface

After the rBMSCs were transfected with the integrin α5- or integrin β1-coding sequence, the mRNA expression level of integrin α5 or β1 increased by 6.5-fold when compared with those of the control or NC groups. The transfection efficiency was confirmed by the doubling in the protein expression level of integrin α5 or integrin β1. No significant difference was identified in the mRNA and protein expression levels between the NC and control groups for the two target genes (Fig. S6B).

When compared with the NC group, up-regulation of integrin α5 elevated the mRNA and protein expression levels of integrin β1 in rBMSCs on the Ti surface at day 1 (about a 1.2-fold increase at the gene level and a 25% increase at the protein level) and vice versa (Fig. 8A, B, G, H). The over-expression of integrin α5 or integrin β1 markedly elevated the gene expression levels of *Erk1, Erk2*, *Runx2*, and *Alp* on the Ti surface (1–2-fold increase; Fig. 8C–F), which was consistent with the 1–2-fold increase in ERK1/2 phosphorylation and more enhanced protein expression of RUNX2 and ALP (Fig. 8G, I, J). Moreover, the enhanced expression of RUNX2 and ALP reached similar or even higher levels than those of the NC group on the Ta surface (Fig. 8E, F, G, I). However, ERK1/2 inhibition abrogated the enhanced mRNA expression of integrin α5, integrin β1, *Runx2*, and *Alp* (Fig. 8A, B, E, F), and the results were verified at the protein level by WB analysis (Fig. 8G, H, I).

rBMSCs with up-regulated integrin α5β1/ERK1/2 signaling maintained higher expression levels of RUNX2 and ALP in comparison to NC on the Ti surface at day 7, and this elevation was also suppressed by ERK1/2 inhibition (Fig. 8E, F; Fig. S7E, G). Furthermore, the interaction among integrin α5, integrin β1, and ERK1/2 induced by the up-regulation of integrin α5 or integrin β1 as well as ERK1/2 inhibition was in accordance with that detected at day 1 (Fig. 8A–D; Fig. S7E, F, H).

The variation of ALP expression on the Ti surface caused by the up- and down-regulation of the integrin α5β1/ERK1/2 pathway was verified by the simultaneous alteration of ALP activity at the corresponding time points (Fig. 8K).

Discussion

Although Ta has been shown to be a superior osteoinducer than Ti [5-10], the underlying mechanism has remained elusive, and the surface modifications and topographical changes applied in many of these studies are also potential routes to induce osteoblastic differentiation [15-17, 28, 29], thereby masking the intrinsic surface effects of Ta and Ti on osteogenesis. Thus, in this study, we addressed this question with a novel approach by using highly polished Ta and Ti substrates to minimize such influences of the surface properties.

Since the Ta and Ti surfaces had a similar influence on cell proliferation, we could eliminate the effect of cell number as a crucial factor influencing the osteoinductive performance of the materials. This finding is consistent with the results of Cortecchia et al [30]., who demonstrated a lack of toxic elements released by the Ta surface in culture medium. Moreover, since the rBMSCs grown in OM, Ta/OM, and Ti/OM, as well as those grown in CM, Ta/CM, and Ti/CM revealed similar ALP activity levels, and the concentrations of Ta or Ti ions were extremely low in both media, we believe that the two substrates exerted a minimal influence on cell osteogenesis through ion release. Alternatively, direct cell–material contact is likely the principal route by which the Ta and Ti substrates affect cell behavior. Given the use of a featureless structure with almost identical nano-scale roughness between the two substrate surfaces, we consider that the surface morphology was not obviously osteoinductive and had similar effects on cell behavior [17-20]. Indeed, the cells showed similar morphology and average spreading areas on the two substrates, which revealed similar influences of topographic guidance on cytoskeleton tension and membrane deformation, as the most important factors regulating cell commitment [31]. There was also no apparent difference in the water contact angles, indicating that the impact of surface

wettability could also be ignored. In consideration of the above findings, it was reasonable to consider that the different osteoinductive performance of the Ta and Ti substrates was mainly determined by the diverse chemical characteristic of their surfaces shown by the XPS analysis.

Although the osteoinductive surrounding provided by OM has been regarded as one of the preconditions for cell osteogenic differentiation *in vitro* [32-34], using a normal culture environment may better reflect the actual effect of a material on osteogenesis; thus, in this study, both OM and CM were adopted for comprehensive testing. In general, cells that grew in CM showed a lower degree of osteoblastic differentiation on the Ta, Ti, and Cp substrates in comparison to those growing on the same substrates in OM. However, within the same medium, rBMSC osteogenesis was markedly enhanced on the Ta surface than that on the Ti and Cp surfaces, as evidenced by the significantly enhanced expression levels of osteoblastic phenotype markers [35] such as RUNX2, ALP, OCN, and COL-I at all time points. RUNX2 is an essential transcription factor for many of the signaling cascades involved in cell osteogenesis [35, 36], and ALP mediates phosphate metabolism via the hydrolysis of phosphate esters and functions as an early marker for osteogenic differentiation [37]. COL-I and OCN are the main ECM proteins in the bones and are crucial indicators of the middle and late stages of osteogenesis [38, 39]. Thus, our results clearly demonstrate that, without contributions of specific surface treatments, the Ta surface not only has a better effect at promoting rBMSC osteogenesis at an early stage but also provides a preferable environment for osteogenesis over the long term. This observation was confirmed by the greater amount of calcium nodules in the ECM on the Ta surface. Our findings are consistent with a previous study using human MSCs, which also showed an elevated degree of ALP activity and ECM mineralization on smooth Ta substrates when compared with those on Ti and chromium substrates [5]. However, our results obtained from cells grown in CM are in contrast with those reported by Findlay and colleagues [3], who found similar osteoinductive capacity between polished Ta and Ti samples. We believe that this discrepancy is mainly due to the diverse surface roughness of the samples applied between the two studies: the surface roughness in the former study (0.29 μm for Ta and 0.37 μm for Ti) was much higher than that of the samples used in our study. As roughness at the submicron level can strongly improve cell osteogenesis when compared with that at the nano-scale [17, 20, 40, 41], the role played by inherent surface effects may have been concealed in the previous study. Moreover, although rBMSCs on the Ti surface had increased ALP expression levels in comparison to those on the Cp surface, the OCN and COL-I secretion levels were almost the same between the two substrates at day 7 and 14, implying that the Ti surface may be conducive to the early stage of cell osteogenesis; however, this effect was relatively short-lived. This finding was in line with the similar ECM calcification rates detected on the two substrates.

Cell–material contact is of great importance in regulating the fate of MSCs, and thus enhancing the expression of the integrin α5β1/mitogen-activated protein kinases 3 and 1 (ERK1/2) pathway is a pivotal mechanism through which a material surface improves MSC osteogenesis [22]. However, the involvement of this pathway in the osteoinductive performance of Ta and Ti had not been verified until now. We found that in both culture media, the production levels of integrin α5, integrin β1, and p-ERK1/2 in rBMSCs on the Ta and Ti surfaces were positively related to their degree of osteoblastic differentiation. Interestingly, the difference in ERK1/2 phosphorylation between the two surfaces in CM was more remarkable than that observed in OM, suggesting that the stimulating effect of a material surface on integrin α5β1/ERK1/2 signaling could be partly overshadowed by components in the OM. This observation may be explained by a previous report by Hamidouche et al. [23], who revealed that the dexamethasone in OM could up-regulate the phosphorylation level of ERK1/2 in MSCs. To eliminate such interference, only CM was used to further assess the role of the integrin α5β1/ERK1/2 cascade in the regulatory mechanisms of the osteoinductive ability of the two surfaces.

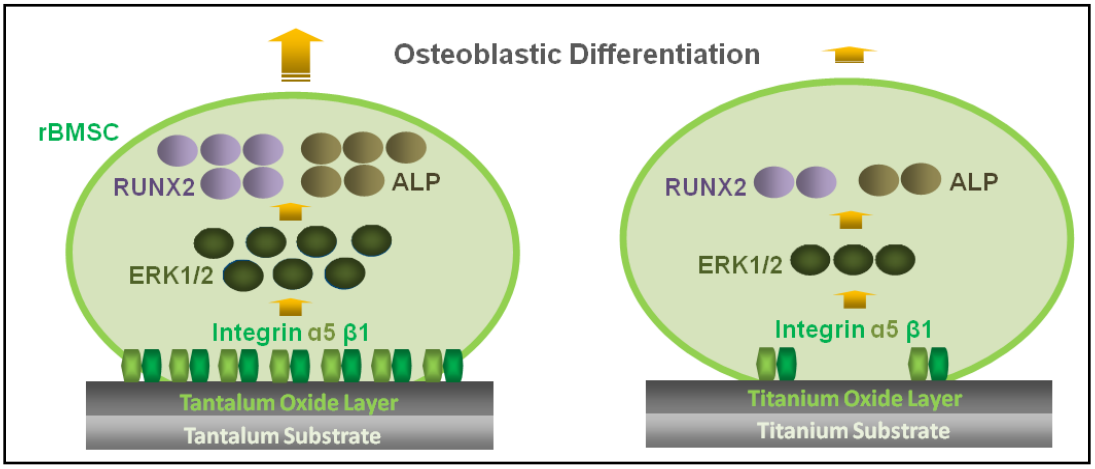

Fig. 9. Possible mechanism of the osteoinductive effect of Ta and Ti surfaces on rBMSCs through the integrin α5β1/ERK1/2 pathway.

Given that knockdown of integrin α5 or integrin β1, or ERK1/2 inhibition, obviously degraded the osteoblastic differentiation on the Ta substrate, we consider that the osteoinductive effect of the Ta surface was greatly alleviated by silencing the integrin α5β1/ERK1/2 pathway. More importantly, the decrease of crucial osteogenic markers reached a similar or even lower level in comparison to those of the negative control group on the Ti surface, indicating that the ability of the Ta surface to more sufficiently activate the integrin α5β1/ERK1/2 signaling pathway may be one of the primary causes of its better osteoinductivity. Similarly, rBMSCs with integrin α5 or integrin β1 over-expression on the Ti surface demonstrated improved osteogenesis, and such improvement reached similar or even a higher level when compared to the negative control on the Ta surface, indicating a close relation between the lower expression of integrin α5β1 and the weak osteoinductive performance of the Ti surface. Moreover, the subsequent application of the ERK1/2 inhibitor U0126 clearly abrogated the enhanced osteogenic differentiation induced by the over-expression of integrin α5 or integrin β1, demonstrating the key role of ERK1/2 in integrin α5β1-mediated osteogenesis. Taken together, these results suggest that the weak osteoinductivity of the Ti surface is, at least partly, attributed to its inadequate capacity to sufficiently trigger the integrin α5β1/ERK1/2 pathway (Fig. 9). Our results further revealed that the down- or up-regulation of integrin α5 could significantly reduce or elevate the expression of integrin β1 and vice versa, and ERK1/2 inhibition markedly lowered the expression levels of integrin α5 and integrin β1, suggesting a feedback control system in which each of these proteins may function as a regulatory molecule to the others in the mediatory work. From another aspect, when compared with those on the Cp surface, rBMSCs on the Ti surface showed enhanced expression of integrin α5β1/ERK1/2 signaling markers, along with a concomitant increase in ALP expression and activity. These parallel changes also validated the mediatory role of the integrin α5β1/ERK1/2 pathway on the two surfaces. By contrast, the similarity of the two surfaces regarding RUNX2 expression at day 14 as well as secretion of OCN and COL-I was in agreement with their similar osteoinductive effects. Thus, further studies are needed to clarify the weaker correlation between the expression of integrin α5β1/ERK1/2 signaling and the difference in the osteoinductivity of Ti and Cp surfaces.

From a material point of view, the surface oxide layers on the Ta and Ti substrates, evidenced by the XPS analysis, may also play a major role in determining the osteogenic fate of rBMSCs. Ti oxides and Ta oxides are well known semiconductors, with a band gap of 3.2 eV and 4.4 eV, respectively [42, 43]. Moreover, the transmembrane proteins in cells (such as integrin α5 and β1 subunits) also behave as semiconductors in wet states, and their band gaps are approximately 3.0 eV [44, 45]. When rBMSCs are spread on polished Ta

and Ti substrates, and the integrin α5β1 makes contact with the surface oxide layer of the substrates, the electron transfer between integrin α5β1 and Ti oxide (i.e., the Ti surface) might be easier than that occurring between integrin α5β1 and Ta oxide (i.e., the Ta surface) because of the band gap difference (3.0 eV vs. 3.2 eV for the former, and 3.0 eV vs. 4.4 eV for the latter) and related band alignment for the couples [42]. This might lead to dysfunction in contact between integrin α5β1 and the Ti surface while contact with the Ta surface was retained, explaining the better osteogenic potential of Ta detected in the present study.

Many studies have revealed a multitude of factors such as mechanical stress [24, 46], anabolic molecules [47, 48], and implant surface topography [49] that can regulate cell osteogenesis through the integrin α5β1 pathway. Our study further demonstrates that the integrin α5β1 signaling cascade is another influencing factor depending on the chemical property of material surfaces. Although a Ta surface may better stimulate integrin α5β1/ERK1/2 signaling in comparison to a Ti surface, in-depth studies are needed to elucidate the specific cause of this effect. Furthermore, as another downstream effector of integrin α5β1, the phosphatidylino-sitol-3-kinase (PI3K)/protein kinase B (AKT) cascade also participate in MSC osteogenesis by regulating cell survival [22]. Therefore, studies focusing on the role of the integrin α5β1/PI3K/AKT cascade on the Ta surface should be carried out to further clarify the molecular mechanism explaining the better osteoinductivity of Ta.

Conclusion

This study demonstrated that the osteoinductivity determined by the intrinsic surface effect of Ta is superior to that of Ti by comparing rBMSCs osteogenesis on smooth Ta and Ti substrates. We found that the integrin α5β1/ERK1/2 signaling cascade plays an important role in regulating rBMSCs osteoblastic differentiation, and that Ta has better ability to activate integrin α5β1/ERK1/2 signaling through cell–material contact than Ti. This may be one of the primary molecular mechanisms underlying the better promoting effect of Ta on cell osteogenesis. Moreover, the different osteoinductive performance between Ta and Ti may be related to the chemical characteristics of their respective surface oxide layers. These findings are expected to enrich knowledge about modification or biofunctionalization of Ta and Ti implants to accomplish better clinical performance.

Acknowledgements

This work was jointly supported by the National Natural Science Foundation of China (31370962, 31670980, 31400825, 81470714, 81870806 and 81800935), Shanghai Rising-Star Program (15QA1404100), Shanghai Committee of Science and Technology (15410722600 and 17441904000), Youth Innovation Promotion Association CAS (2015204), Innovation Fund of Translational Medicine of Medicine School of Shanghai Jiaotong University (15ZH2012), Shanghai Pujiang Program (17PJD030), and Collaborative Research Program of Collaborative Innovation Center in Translational Medicine (TM201819).

Disclosure Statement

The authors have not conflicts of interest to declare.

References

1 Geetha M, Singh AK, Asokamani R, Gogia AK: Ti based biomaterials, the ultimate choice for orthopaedic implants-a review. Prog Mater Sci 2009;54:397–425.

2 Levine BR, Sporer S, Poggie RA, Della Valle CJ, Jacobs JJ: Experimental and clinical performance of porous tantalum in orthopedic surgery. Biomaterials 2006;27:4671–4681.

3 Findlay DM, Welldon K, Atkins GJ, Howie DW, Zannettino AC, Bobyn D: The proliferation and phenotypic expression of human osteoblasts on tantalum metal. Biomaterials 2004;25:2215–2227.

4 Myllymaa S, Kaivosoja E, Myllymaa K, Sillat T, Korhonen H, Lappalainen R, Konttinen YT: Adhesion, spreading and osteogenic differentiation of mesenchymal stem cells cultured on micropatterned amorphous diamond, titanium, tantalum and chromium coatings on silicon. J Mater Sci Mater Med 2010;21:329–341.

5 Stiehler M, Lind M, Mygind T, Baatrup A, Dolatshahi-Pirouz A, Li H, Foss M, Besenbacher F, Kassem M, Bünger C: Morphology, proliferation, and osteogenic differentiation of mesenchymal stem cells cultured on titanium, tantalum, and chromium surfaces. J Mater Sci Mater Med 2010;21:329–341.

6 Tang Z, Xie Y, Yang F, Huang Y, Wang C, Dai K, Zheng X, Zhang X: Porous tantalum coatings prepared by vacuum plasma spraying enhance bmscs osteogenic differentiation and bone regeneration *in vitro* and *in vivo*. PLoS One 2013;8:e66263.

7 Wang L, Hu X, Ma X, Ma Z, Zhang Y, Lu Y, Zheng X, Zhang X: Promotion of osteointegration under diabetic conditions by tantalum coating-based surface modification on 3-dimensional printed porous titanium implants. Colloids Surf B Biointerf 2016;148:440–452.

8 Li X, Wang L, Yu X, Feng Y, Wang C, Yang K, Su D: Tantalum coating on porous Ti6Al4V scaffold using chemical vapor deposition and preliminary biological evaluation. Mater Sci Eng C Mater Biol Appl 2013;33:2987–2994.

9 Matsuno H, Yokoyama A, Watari F, Uo M, Kawasaki T: Biocompatibility and osteogenesis of refractory metal implants, titanium, hafnium, niobium, tantalum and rhenium. Biomaterials 2001;22:1253–1262.

10 Wauthle R, van der Stok J, Amin Yavari S, Van Humbeeck J, Kruth JP, Zadpoor AA, Weinans H, Mulier M, Schrooten J: Additively manufactured porous tantalum implants. Acta Biomater 2015;14:217–225.

11 Habibovic P, de Groot K: Osteoinductive biomaterials--properties and relevance in bone repair. J Tissue Eng Regen Med 2007;1:25–32.

12 Olivares-Navarrete R, Hyzy SL, Hutton DL, Erdman CP, Wieland M, Boyan BD, Schwartz: Direct and indirect effects of microstructured titanium substrates on the induction of mesenchymal stem cell differentiation towards the osteoblast lineage. Biomaterials 2010;31:2728–2735.

13 Frandsen CJ, Brammer KS, Noh K, Johnston G, Jin S: Tantalum coating on TiO2 nanotubes induces superior rate of matrix mineralization and osteofunctionality in human osteoblasts. Mater Sci Eng C Mater Biol Appl 2014;37:332–341.

14 Sagomonyants KB, Hakim-Zargar M, Jhaveri A, Aronow MS, Gronowicz G: Porous tantalum stimulates the proliferation and osteogenesis of osteoblasts from elderly female patients. J Orthop Res 2011;29:609–616.

15 Di Cio S, Gautrot JE: Cell sensing of physical properties at the nanoscale: Mechanisms and control of cell adhesion and phenotype. Acta Biomater 2016;30:26–48.

16 Huri PY, Ozilgen BA, Hutton DL, Grayson WL: Scaffold pore size modulates *in vitro* osteogenesis of human adipose-derived stem/stromal cells. Biomed Mater 2014;9:045003.

17 Rosa AL, Beloti MM: Rat bone marrow cell response to titanium and titanium alloy with different surface roughness. Clin Oral Implants Res 2003;14:43–48.

18 Bachle M, Kohal RJ: A systematic review of the influence of different titanium surfaces on proliferation, differentiation and protein synthesis of osteoblast-like MG63 cells. Clin Oral Implants Res 2003;14:43–48.

19 Mustafa K, Wennerberg A, Wroblewski J, Hultenby K, Lopez BS, Arvidson K: Determining optimal surface roughness of TiO(2) blasted titanium implant material for attachment, proliferation and differentiation of cells derived from human mandibular alveolar bone. Clin Oral Implants Res 2001;12:515–525.

20 Rosa AL, Beloti MM: Effect of cpTi surface roughness on human bone marrow cell attachment, proliferation, and differentiation. Braz Dent J 2003;14:16–21.

21 Boyan BD, Cheng A, Olivares-Navarrete R, Schwartz Z: Implant surface design regulates mesenchymal stem cell differentiation and maturation. Adv Dent Res 2016;28:10–17.

22 Marie PJ: Targeting integrins to promote bone formation and repair. Nat Rev Endocrinol 2013;9:288–295.

23 Hamidouche Z, Fromigue O, Ringe J, Haupl T, Vaudin P, Pages JC, Srouji S, Livne E, Marie PJ: Priming integrin alpha5 promotes human mesenchymal stromal cell osteoblast differentiation and osteogenesis. Proc Natl Acad Sci USA 2009;106:18587–18591.
24 Dufour C, Holy X, Marie PJ: Skeletal unloading induces osteoblast apoptosis and targets alpha5beta1-PI3K-Bcl-2 signaling in rat bone. Exp Cell Res 2007;313:394–403.
25 Fromigue O, Brun J, Marty C, Da Nascimento S, Sonnet P, Marie PJ: Peptide-based activation of alpha5 integrin for promoting osteogenesis. J Cell Biochem 2012;113:3029–3038.
26 Shen Q, Zeng D, Zhou Y, Xia L, Zhao Y, Qiao G, Xu L, Liu Y, Zhu Z, Jiang X: Curculigoside promotes osteogenic differentiation of bone marrow stromal cells from ovariectomized rats. J Pharm Pharmacol 2013;65:1005–1113.
27 Kemp KC, Hows J, Donaldson C: Bone marrow-derived mesenchymal stem cells. Leuk Lymph 2005;46:1531–1544.
28 Balla VK, Banerjee S, Bose S, Bandyopadhyay A: Direct laser processing of a tantalum coating on titanium for bone replacement structures. Acta Biomater 2010;6:2329–2334.
29 Ninomiya JT, Struve JA, Krolikowski J, Hawkins M, Weihrauch D: Porous ongrowth surfaces alter osteoblast maturation and mineralization. J Biomed Mater Res A 2015;103:276–281.
30 Cortecchia E, Pacilli A, Pasquinelli G, Scandola M: Biocompatible two-layer tantalum/titania-polymer hybrid coating. Biomacromolecules 2010;11:2446–2453.
31 Ozdemir T, Higgins AM, Brown JL: Osteoinductive biomaterial geometries for bone regenerative engineering. Curr Pharm Des 2013;19:3446–3455.
32 Frank O, Heim M, Jakob M, Barbero A, Schafer D, Bendik I, Dick W, Heberer M, Martin I: Real-time quantitative RT-PCR analysis of human bone marrow stromal cells during osteogenic differentiation *in vitro*. J Cell Biochem 2002;85:737–746.
33 Langenbach F, Handschel J: Effects of dexamethasone, ascorbic acid and beta-glycerophosphate on the osteogenic differentiation of stem cells *in vitro*. Stem Cell Res Ther 2013;4:117.
34 Wang W, Zhao L, Ma Q, Wang Q, Chu PK, Zhang Y: The role of the Wnt/beta-catenin pathway in the effect of implant topography on MG63 differentiation. Biomaterials 2012;33:7993–8002.
35 Li Y, Jiang T, Zheng L, Zhao J: Osteogenic differentiation of mesenchymal stem cells (MSCs) induced by three calcium phosphate ceramic (CaP) powders: a comparative study. Mater Sci Eng C Mater Biol Appl 2017;80:296–300.
36 Ducy P, Zhang R, Geoffroy V, Ridall AL, Karsenty G: Osf2/Cbfa1: a transcriptional activator of osteoblast differentiation. Cell 1997;89:747–754.
37 Whyte MP: Hypophosphatasia and the role of alkaline phosphatase in skeletal mineralization. Endocr Rev 1994;15:439–461.
38 Viguet-Carrin S, Garnero P, Delmas PD: The role of collagen in bone strength. Osteoporos Int 2006;17:319–336.
39 Wada S, Fukawa T, Kamiya S: Osteocalcin and bone. Clin Calcium 2007;17:1673–1677.
40 Deligianni DD, Katsala N, Ladas S, Sotiropoulou D, Amedee J, Missirlis YF: Effect of surface roughness of the titanium alloy Ti-6Al-4V on human bone marrow cell response and on protein adsorption. Biomaterials 2001;22:1241–1251.
41 Kim HJ, Kim SH, Kim MS, Lee EJ, Oh HG, Oh WM, Park SW, Kim WJ, Lee GJ, Choi NG, Koh JT, Dinh DB, Hardin RR, Johnson K, Sylvia VL, Schmitz JP, Dean DD: Varying Ti-6Al-4V surface roughness induces different early morphologic and molecular responses in MG63 osteoblast-like cells. J Biomed Mater Res A 2005;74:366–373.
42 Chen JY, Leng YX, Tian XB, Wang LP, Huang N, Chu PK, Yang P: Antithrombogenic investigation of surface energy and optical bandgap and hemocompatibility mechanism of Ti(Ta(+5))O2 thin films. Biomaterials 2002;23:2545–2552.
43 Robertson J, Chen CW: Schottky barrier heights of tantalum oxide, barium strontium titanate, lead titanate, and strontium bismuth tantalate. Appl Phys Lett 1999;74:1168–1170.
44 Alexson D, Chen H, Cho M, Dutta M, Li Y, Shi P, Raichura A, Ramadurai D, Parikh S, Stroscio MA, Vasudev M: Semiconductor nanostructures in biological applications. J Phys Condens Matter 2005;17:R637.
45 Rosenberg B: Electrical conductivity of proteins. Nature 1962;193:364–365.
46 Watabe H, Furuhama T, Taniishii N, Yexcr J: Mechanotransduction activates alpha(5)beta(1) integrin and PI3K/Akt signaling pathways in mandibular osteoblasts. Exp Cell Res 2011;317:2642–2649.

47 Nesti LJ, Caterson EJ, Wang M, Chang R, Chapovsky F, Hoek JB, Tuan RS: TGF-beta1 calcium signaling increases alpha5 integrin expression in osteoblasts. J Orthop Res 2002;20:1042–1049.
48 Park SJ, Gadi J, Cho KW, Kim KJ, Kim SH, Jung HS, Lim SK: The forkhead transcription factor Foxc2 promotes osteoblastogenesis via up-regulation of integrin beta1 expression. Bone 2011;49:428–438.
49 Lee JS, Yi JK, An SY, Heo JS: Increased osteogenic differentiation of periodontal ligament stem cells on polydopamine film occurs via activation of integrin and PI3K signaling pathways. Cell Physiol Biochem 2014;34:1824–1834.